DOI: 10.1002/ejoc.200801001

NMR Enantiodiscrimination Phenomena by Quinine C^9-Carbamates

Gloria Uccello-Barretta,*[a] Letizia Vanni,[a] and Federica Balzano[a]

Keywords: Chirality / Chiral recognition / Chiral auxiliaries / Enantiomeric purity / NMR spectroscopy

Several C^9-carbamoyl derivatives of quinine have been prepared and compared as chiral solvating agents in NMR enantiodiscrimination experiments of amino acid derivatives. The origin of the enantiodiscrimination phenomena was identified by NMR conformational analysis of the chiral auxiliaries and investigations of solution complexation phenomena.

Introduction

Cinchona alkaloids, and quinine (**1**, Figure 1) in particular, represent remarkably powerful and versatile chiral auxiliaries by virtue of the presence of different functional groups that are able to fit the stereochemical requirements of several classes of compounds in molecular and chiral recognition processes. Furthermore, their enantiodiscriminating properties can be modulated and effectively addressed by derivatization processes. Quinine C^9-carbamates, which can be obtained by a very simple modification of the quinine hydroxy group, have found widespread applications in asymmetric synthesis or catalysis,[1] as well as in the analytical and/or preparative separations of enantiomers.[2,3] With regard to NMR spectroscopy, some quinine C^9-carbamates have been successfully employed as chiral solvating agents (CSAs)[2] to induce differentiation of NMR-active nuclei of enantiomeric mixtures and hence afford an efficient complementary approach to their direct analytical separation by chromatographic methods.[3]

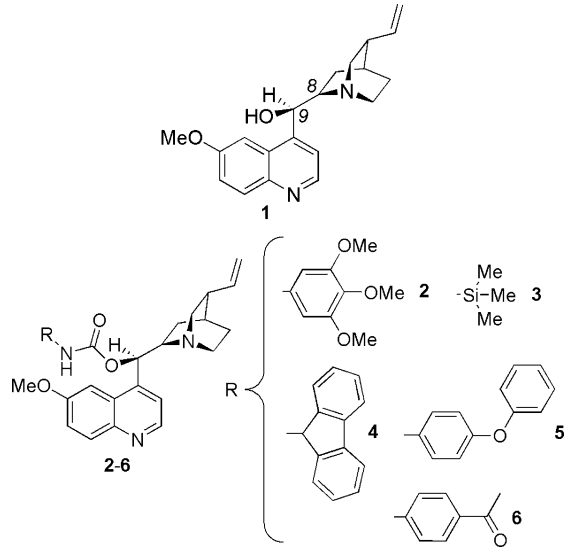

Figure 1. Chiral solvating agents **1**–**6**.

The important applications of the quinine C^9-carbamates prompted us to ascertain the role of the moiety bound to the carbamate function in NMR enantiorecognition processes that occur in solution. With this aim we synthesized different new quinine C^9-carbamates **2**–**6** (Figure 1) to be employed as chiral complexing agents in NMR experiments and probed their enantiodiscriminating efficiency towards *N*-trifluoroacetyl derivatives of amino acids with a free carboxy function **7**–**11** (Figure 2) in comparison with derivatives **12**–**14**. Amino acid derivatization, as in the synthesis of **7**–**11**, is remarkably advantageous from a preparative point of view as the reaction involved is very simple, quick and no time-consuming purification procedures are needed. And importantly, it provides an opportunity to detect enantiodiscrimination by ^{19}F NMR experiments.

Owing to the fact that quinine has a very high degree of structural preorganization, which could be affected significantly by derivatization processes, we correlated conformational features of **2**–**6** with their enantiodiscriminating ability and compared their stereochemical and dynamics features in the absence and in the presence of enantiomeric substrates with the final goal of gaining a greater insight into the origin of enantiodiscrimination processes and hence get to the root of chiral recognition mechanisms involving quinine C^9-carbamates. Investigations were carried out by using complementary NMR techniques including extensive use of DOSY (Diffusion Ordered SpectroscopY)[4] spectroscopy.

[a] Università degli Studi di Pisa, Dipartimento di Chimica e Chimica Industriale,
Via Risorgimento 35, 56126 Pisa, Italy
Fax: +39-0502219260
E-mail: gub@dcci.unipi.it

Supporting information for this article is available on the WWW under http://www.eurjoc.org or from the author.

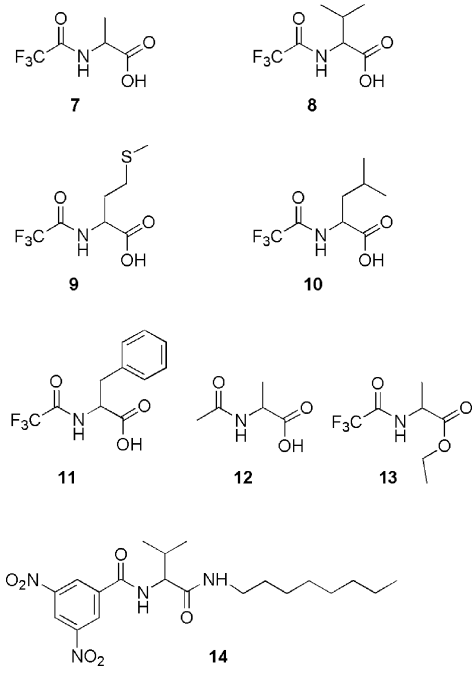

Figure 2. α-Amino acid derivatives **7**–**14**.

Results and Discussion

Derivatives **2**–**6** were prepared by the treatment of quinine with the appropriate isocyanate and characterized by a combined use of 2D NMR techniques (see the Exptl. Sect.).

^{1}H and ^{19}F NMR Enantiodiscrimination Experiments

NMR enantiodiscrimination experiments were carried out in $CDCl_3$ by comparison of the spectra of pure 5 mM chiral substrates **7**–**12** and their equimolar mixtures with **1**–**6**. ^{1}H NMR non-equivalences (differences between the chemical shifts of the two enantiomers in the presence of the chiral auxiliary) for alanine derivative **7** are summarized in Table 1. The methyl protons of **7** were differentiated to a greater extent by quinine carbamates than the underivatized alkaloid (Figure 3); anisochrony of the methine nucleus was induced only by carbamates and chiral auxiliaries did not produce a doubling of the amide resonances. However, of the carbamoyl derivatives, the trimethylsilyl **3** and the fluorenyl **4** derivatives showed the highest enantiodiscriminating efficiencies as the non-equivalences for the methyl and methine groups of **7**, respectively, were 0.035 and 0.037 ppm in the mixture containing **3** and 0.027 ppm (for both methyl and methine groups) in the presence of **4**, which compares with non-equivalences of less than 0.02 ppm in mixtures containing the other carbamates.

Interestingly, underivatized quinine **1** and its carbamate derivatives **2**–**6** caused remarkable low-frequency shifts of the methyl (Figure 3) and methine resonances (Table 1) together with remarkable high-frequency shifts of the amide resonance (Table 1). Analysis of analogous mixtures containing enantiomerically enriched samples of **7** showed that the shielding effect of alkyl protons was more pronounced for (*S*)-**7** than it was for (*R*)-**7** (Figure 3).

Table 1. ^{1}H NMR (600 MHz, $CDCl_3$, 25 °C) complexation shifts[a] and the non-equivalences[b] of **7** (5 mM) in the presence of equimolar amounts of **1**–**6**.

	Me		CH		NH	
	$\delta_{mix} - \delta_{free}$	$\Delta\delta$	$\delta_{mix} - \delta_{free}$	$\Delta\delta$	$\delta_{mix} - \delta_{free}$	$\Delta\delta$
7/1	–0.05 (*R*) –0.06 (*S*)	0.013	–0.32	0	0.68	0
7/2	–0.04 (*R*) –0.06 (*S*)	0.021	–0.32 (*R*) –0.30 (*S*)	0.020	0.68	0
7/3	–0.01 (*R*) –0.05 (*S*)	0.035	–0.41 (*R*) –0.37 (*S*)	0.037	n.d.[c]	n.d.[c]
7/4	–0.01 (*R*) –0.04 (*S*)	0.027	–0.28 (*R*) –0.26 (*S*)	0.027	0.70	0
7/5	–0.05 (*R*) –0.06 (*S*)	0.019	–0.27 (*R*) –0.26 (*S*)	0.013	0.53	0
7/6	–0.05 (*R*) –0.06 (*S*)	0.018	–0.25	0	n.d.[c]	n.d.[c]

[a] $\delta_{mix} - \delta_{free}$, where δ_{mix} = the chemical shift in the mixture and δ_{free} = the chemical shift of the pure compound (measured in ppm). [b] $\Delta\delta = |\delta_R - \delta_S|$ (measured in ppm). [c] n.d. = not determined.

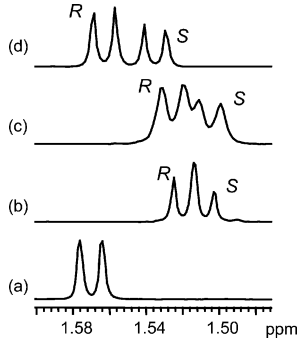

Figure 3. ^{1}H NMR (600 MHz, $CDCl_3$, 25 °C, 5 mM) spectral regions corresponding to the methyl resonance of **7** enantiomerically enriched in the *R* enantiomer alone (a) and in the presence of equimolar amounts of **1** (b), **2** (c) and **4** (d).

The derivative of valine **8** showed an analogous response to the presence of quinine **1** and the quinine carbamates (Table 2, Figure 4): with the exception of **6**, the carbamates caused a more efficient differentiation of the alkyl protons of enantiomers of **8** compared with the underivatized quinine. Differentiation of its amide resonance was not detected. Of the carbamates, **3** and **4** allowed us to measure the highest non-equivalences (Table 2, Figure 4). In any case, the alkyl protons and amide proton were, respectively, low- and high-frequency shifted in the mixtures relative to pure **8**.

As a general trend, carbamates **3** and **4** were able to differentiate efficiently alkyl protons of enantiomeric mixtures of methionine (**9**), leucine (**10**) and phenylalanine (**11**) derivatives (Table S1, Supporting Information).

Table 2. Non-equivalences[a] (600 MHz, 25 °C, $CDCl_3$) of the methine proton of substrate **8** (5 mM) and **14** (15 mM) in the presence of equimolar amounts of **1**–**6**.

	$\Delta\delta$ [ppm]		$\Delta\delta$ [ppm]
8/1	0.014	**14/1**	0.002
8/2	0.017	**14/2**	0.005
8/3	0.039	**14/3**	0
8/4	0.041	**14/4**	0
8/5	0.022	**14/5**	0.005
8/6	0.010	**14/6**	0

[a] $\Delta\delta = |\delta_R - \delta_S|$.

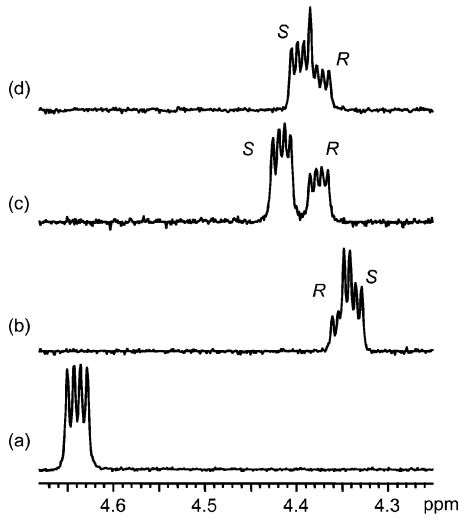

Figure 4. ^1H NMR (600 MHz, $CDCl_3$, 25 °C, 5 mM) spectral regions corresponding to the methine resonance of **8** enantiomerically enriched in the *S* enantiomer, alone (a) and in the presence of equimolar amounts of **1** (b), **4** (c) and **5** (d).

The presence of a trifluoromethyl group did not seem to be a prerequisite for enantiodiscrimination by carbamates as both the methyl and methine protons of the *N*-acetyl derivative of alanine **12** were differentiated in the presence of carbamates (Table 3).

Table 3. Non-equivalences[a] (600 MHz, 25 °C, $CDCl_3$) of **12** (5 mM) in presence of equimolar amounts of **1**–**6**.

	$\Delta\delta$ [ppm]		
	Me	CH	NH
12/1	0.012	0	0
12/2	0.024	0	0
12/3	0.017	0.039	0.016
12/4	0.021	0.011	0
12/5	0.016	0.009	0.011
12/6	0.021	0.011	0

[a] $\Delta\delta = |\delta_R - \delta_S|$.

The presence of a free carboxy function is fundamental for efficient enantiodiscrimination as differentiation of enantiomeric signals of the ester derivative of alanine **13** was detected only at significantly higher equimolar concentrations of the substrate and carbamate (60 mM) and also under these conditions the non-equivalences were quite low. The presence of a different acidic group, as in the diamide derivative **14** (Figure 2), made it possible to measure non-equivalences, but the enantiodiscriminating efficiency was lower than it was for **8** (Table 2) in which an amide and a free carboxy function are present.

Finally, as most of the substrates analysed (**7**–**11** and **13**, Figure 2) contain fluorine atoms, we could also analyse the ^{19}F NMR spectra of their equimolar mixtures with **1**–**6**. In this regard it is important to emphasize that observing ^{19}F nuclei represents a very interesting approach because any interference from CSA resonances is removed and also because, in the presence of low non-equivalences, accurate enantiomeric purity determinations can be performed. In fact, ^{19}F NMR enantiomeric signals of *N*-trifluoromethyl groups are singlets and enantiomeric excesses can be measured by comparison both of the integrated areas and of the peaks heights. This is true on the basis that resonance differentiation arises from the interaction of enantiomeric substrates with diamagnetic chiral auxiliaries. The *N*-trifluoromethyl group of **7** gave a ^{19}F NMR signal at –13.58 ppm, which doubled into two low-frequency shifted signals in the presence of each carbamate derivative (non-equivalences of about 0.01 ppm) with the sole exception of CSA **5** (Table S2, Supporting Information). Underivatized quinine **1** did not cause differentiation of fluorine resonances (Table S2, Supporting Information). The enantiomeric purity of a sample of (*R*)-**7** (optical purity 20.1%) was determined by comparing integrated areas of the two signals (19.8%) and their signal heights (20.1%) with its known value. The accuracy of the enantiomeric purity determination was also checked for the valine derivative **8**, enantiomeric fluorine signals of which were differentiated only by carbamate derivatives with higher non-equivalences in the presence of **4** (Table S2, Supporting Information). Even higher non-equivalences (Figure 5) were measured in the case of the phenylalanine derivative **11** (0.032 ppm in the presence of **3** and 0.027 ppm in the presence of **4**), whereas, surprisingly, no non-equivalence of the fluorinated group in the methionine derivative **9** was measured (see Supporting Information, Table S3). The fluorine signals of all the substrates were low-frequency shifted in mixtures containing the chiral auxiliaries compared with the pure compounds.

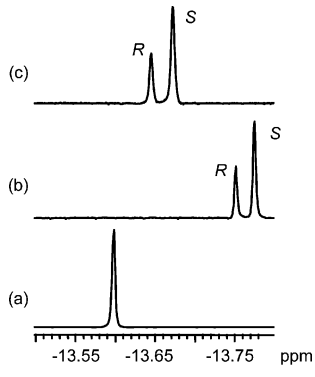

Figure 5. ^{19}F NMR (564 MHz, $CDCl_3$, 25 °C, 5 mM) spectra of substrate **11** alone (a) and in the presence of equimolar amounts of **3** (b) and **4** (c).

Conformational Analysis of Chiral Auxiliaries 2–6

Even though, in principle, the interaction with enantiomeric substrates could bring about important conformational changes of the chiral auxiliary, the role of the stereochemical preorganization of chiral auxiliaries is recognized in both their enantiodiscriminating efficiency and their versatility. Thus, as the starting point for the rationalization of chiral recognition processes, the conformation of each chiral auxiliary was investigated. With this aim, the relative orientations of the quinoline and quinuclidine moieties and the stereochemistry of the carbamate moiety with respect to the main quinine skeleton were defined.

Rotations about the C8–C9 and C9–C16 bonds (Figure 6) can lead to several conformers, among which the more populated ones (at least at room temperature) are depicted for cinchonidine[5] in Figure 6 and named as Closed(1), Closed(2), Open(3) and Open(4).

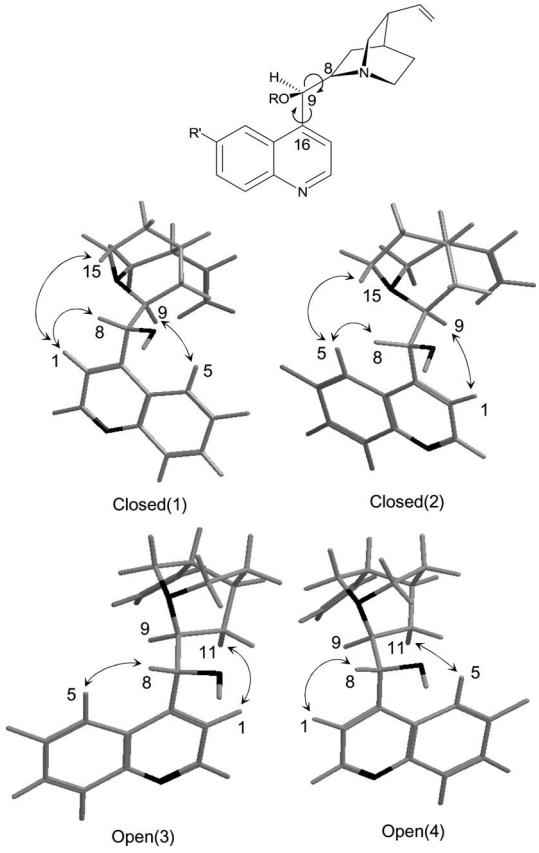

Figure 6. Graphical representation of the conformers of cinchonidine.[5]

The H8–C9–O and quinuclidine moieties of all the limiting conformers lie on opposite sides with respect to the quinoline ring. In the closed conformers the quinuclidine nitrogen points towards the quinoline ring, whereas in the open conformers it is far away from it, which corresponds to dihedral angles H8–C9–C8–H9 close to –180 and –80°, respectively. In the Closed(1)/Open(4) conformers, proton H8 points towards the quinoline H1 proton, whereas in the Closed(2)/Open(3) conformers the same proton is directed at the quinoline H5 proton. Such well-defined stereochemical differentiation of the four conformers makes it possible not only to identify qualitatively the average conformation in solution by detecting through-space internuclei dipole–dipole interactions by NOE (nuclear Overhauser effect) or ROE (rotating-frame Overhauser enhancement) methods, but also to determine the relative amounts of the four conformers. Thus, for each chiral auxiliary we initially detected the relevant ROE interactions by 1D or 2D ROESY experiments to determine the nature of the more populated conformers. Then their relative amounts were determined by analysing the dependence of the vicinal coupling constants $^3J_{89}$ on the dihedral angle between the H9–C8–C9 and H8–C9–C8 planes. ROE experiments were carried out in place of NOE ones as a slow motion regime ($\omega^2\tau_c^2 >> 1$, where ω is the Larmor frequency and τ_c is the reorientational correlation time) led to negative NOEs.

The 1D ROESY spectrum (Figure 7, a) of the carbamate derivative **2** bearing a 3,4,5-trimethoxyphenyl moiety clearly showed that on average the H8 proton is nearer to the H5 quinoline proton than it is to H1, which suggests the prevalence of the Closed(2) and Open(3) conformers. Negligible amounts of the Closed(1) conformer are indicated by a very low intensity H1–H15 ROE (Figure 7, b) and an undetectable H5–H11 ROE confirms the nearly complete absence of the Open(4) conformer. The Closed(2) conformer must prevail strongly over Open(3) due to the fact that the H1–H11 ROE (Figure 7, b) is significantly less intense than the H1–H9 ROE. The prevalence of the Closed(2) conformer is also clearly evidenced by comparison of the H8–H15 and H8–H9 ROEs, with the first more intense than the latter (Figure 7, a).

In the ^{1}H NMR spectrum of **2** we measured a value of 7.3 Hz for the vicinal coupling constant $^3J_{89}$ between protons H8 and H9 (Table 4). This parameter, which represents the weighted average of the corresponding values $^3J_{89}{}^i$ of the conformers, can be expressed by Equation (1), in which $P_{(i)}$ refers to the populations of the Closed(1), Closed(2), Open(3) and Open(4) conformers and $^3J_{89}{}^i$ the correspond-

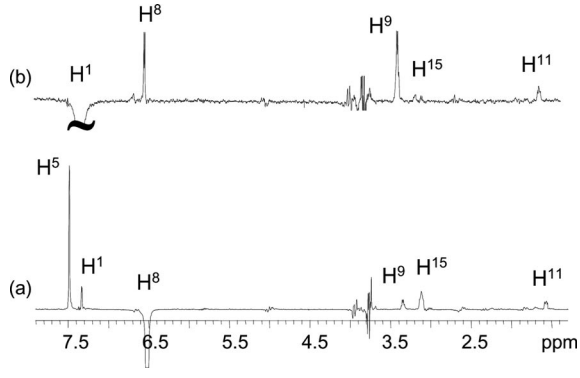

Figure 7. 1D ROESY spectra (600 MHz, $CDCl_3$, 75 mM, 25 °C, mix 0.6 s) corresponding to the selective inversion of the H8 (a) and H1 (b) protons of **2**.

ing expected vicinal coupling constants, which were assumed to be equal to the values reported by Burgi and Baiker.[5]

$$^3J_{89} = \Sigma_i[P_{(i)}{}^3J_{89}{}^i] \quad (1)$$

Table 4. ^{1}H NMR chemical shifts (600 MHz, $CDCl_3$, 25 °C, 75 mM) for the H1, H5 and H8 protons and the $^3J_{89}$ coupling constants for compounds **1**–**6**.

	δ_H [ppm]			$^3J_{89}$ [Hz]
	H1	H5	H8	
1	7.49	7.24	5.47	2.9
2	7.33	7.48	6.51	7.3
3	7.48	7.19	5.67	n.d.[a]
4	7.38	7.53	6.60	6.6
5	7.41	7.49	6.53	8.3
6	7.38	7.49	6.54	7.5

[a] Not determined.

Owing to the fact that, on the basis of the ROE data, the Open(4) population can be neglected and $^3J_{89}^{Closed(1)} \cong {}^3J_{89}^{Closed(2)}$, the relative amounts of the Open(3) and Closed(1) + Closed(2) conformers can be calculated by solving Equation (1), in which the sum of the population $P_{(i)}$ is equal to 1.

In this way we obtained for **2** a 72% Closed(2) + Closed(1) population and 28% of the Open(3) conformer (Table 5). The absence of the Open(4) conformer also allowed us to obtain the Closed(1)/Closed(2) ratio from a comparison of the integrated areas of the H1–H15 and H1–H9 ROEs, which was 2:98 (Table 5). Thus, we could conclude that carbamate **2** exists predominantly as the Closed(2) conformer, but a significant amount of the Open(3) conformer was present.

A similar analysis of the 1D ROESY spectrum (Figure S1, Supporting Information) and the H8–H9 vicinal coupling constant (Table 4) of carbamate **4** with a fluorenyl moiety allowed us to confirm the prevalence of the Closed(2) + Closed(1) conformers relative to the Open(3) one, with a negligible contribution from the Open(4) conformer (Table 5). However, the Open(3) population of **4** was higher (37%) than it was for **2** with a significant contribution from the Closed(1) conformer (H1–H15 ROE/H1–H9 ROE = 19:81; Table 5).

Carbamate **6** with a *p*-acetylphenyl moiety was similar (Figure S2, Supporting Information) to carbamate **2** with regard to the ratio between the Open(3) and Closed(1) + Closed(2) conformers, but similar to **4** with regard to the Closed(1)/Closed(2) ratio (Table 5).

Table 5. Population of the conformers for quinine derivatives **2**–**6**.

	$P_{O(3)}$ [%]	$P_{C(1)} + P_{C(2)}$ [%]	H1–H15 ROE/H1–H9 ROE
2	28	72	2:98
3	≈ 50	≈ 50	≈ 0:100
4	37	63	19:81
5	15	85	21:79
6	25	75	20:80

Carbamate **5** with a *p*-phenoxyphenyl group had the lowest population of the Open(3) conformer and a Closed(1)/Closed(2) ratio comparable to those found for **4** and **6** (Table 5).

Finally, conformational analysis of carbamate **3** with the trimethylsilyl moiety was made very difficult by the extensive superimposition of its NMR resonances and by their remarkably broad linewidths. However, a strong indication of its conformation was given by the relative intensities of the H8–H9 and H8–H15 ROEs, which indicated nearly equivalent amounts of the Open(3) and Closed conformers, whereas a high intensity H8–H5 ROE indicated very low amounts both of Closed(1) and Open(4) conformers. Analysis of the vicinal coupling constant $^3J_{89}$ was not possible in this case and thus the populations reported in Table 5 are based on ROE data.

In summary, quinine carbamates preferentially assume Closed(2) conformations, but the nature of the carbamate function is able to affect significantly the amount of the Open(3) conformer, the quinuclidine nitrogen of which is more predisposed to originate attractive interactions with acidic enantiomeric substrates, at least in principle. As described above, the Open conformer population increases from a minimum value of about 15% in the case of **5** to 25 and 28% for **6** and **2**, respectively, with very large amounts present in **3** and **4** (Table 5).

The carbamate moiety must lie far from the quinuclidine or quinoline groups with the C9–H8 and N–H bonds *transoid* as no reciprocal internuclei dipolar interaction was detected over a wide range of mixing times (from 0.05 to 1.2 s) by 1D and 2D ROESY measurements. Thus, the C9–H8 bond should face the carbonyl group, as depicted in Figure 8 for compounds **2**, **5** and **6**, and both the N–H bond and the aromatic moiety are closer to the quinoline portion bearing the H1 and H2 protons and farther from the quinoline portion in which the methoxy group is located. Accordingly, the H1 proton, which would feel the shielding effect of the carbamate aromatic ring, was always low-frequency shifted compared with H5 relative to **1** (Table 4). Derivative **3** with the trimethylsilyl moiety was the sole exception of the trend described above as its H8 proton gave an ROE interaction with the NH proton and, similar to the underivatized quinine, its H5 proton was shifted to a lower frequency than the H1 proton (Table 4), which indicates that in the case of **3**, C9–H8 and N–H are *cisoid* and the trimethylsilyl moiety is closer to the quinoline portion bearing the methoxy group.

In the case of derivative **4** a very weak dipolar interaction was detected between the two vicinal protons N–H and Ha, which, consequently, on average must be *transoid* (Figure 9). The vicinal coupling constant J_{NH-Ha} of 9.4 Hz was then correlated to the dihedral angle of 157.2° by solving the Karplus equation[6] with parameters optimized for such a molecular fragment.

Interestingly, the corresponding protons of the two phenyl rings of the fluorenyl group, which were isochronous in the starting isocyanate, were differentiated once bound to the alkaloid, which indicates hindered rotation about the

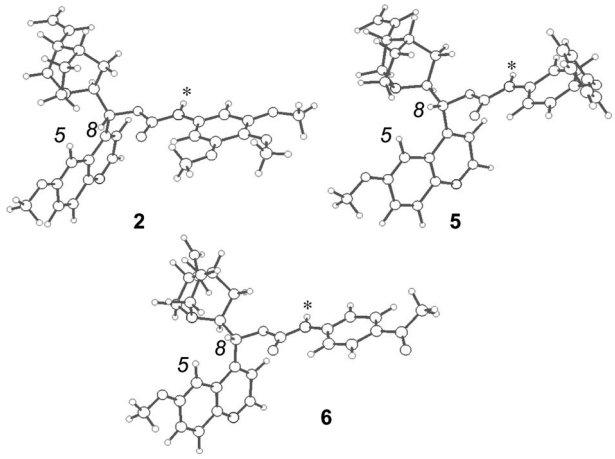

Figure 8. Graphical representation of the average conformations of derivative **2**, **5** and **6** in $CDCl_3$ solution (* hydrogen atom bound to the nitrogen atom of the carbamoyl function).

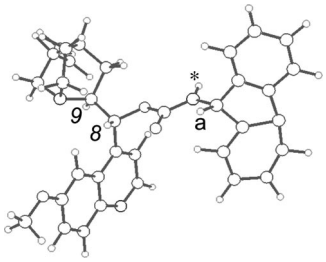

Figure 9. Graphical representation of the average conformation of derivative **4** in $CDCl_3$ solution (* hydrogen atom bound to the nitrogen atom of the carbamoyl function).

N–C bond. Note, all the protons of one of the phenyl groups of the fluorenyl are low-frequency shifted (Hb/Hc/Hd/He, see the Exptl. Sect.) with respect to the proton nuclei on the second (Hb′/Hc′/Hd′/He′), probably being closer to and farther from the quinoline moiety, respectively. This last hypothesis could not be confirmed by ROE measurements as no dipolar interactions between the fluorenyl and quinoline moieties were detected.

Study of the Enantiodiscrimination Mechanism

In our investigation into the origin of enantiodiscrimination processes, we first considered the possible occurrence of self-association phenomena of chiral selectors, which were previously detected in underivatized quinine[7] and, in principle, could reduce the availability of some functional groups required for enantiorecognition.

DOSY spectroscopy represents a very powerful tool for detecting supramolecular aggregation phenomena as it allows us to measure translational diffusion coefficients D, which are size-dependent parameters by virtue of their inverse dependence on hydrodynamic radii R_H and hence molecular sizes and are given by the Stokes–Einstein equation [Equation (2),[4] in which k represents the Boltzmann constant, T the absolute temperature and η the solution viscosity, which can be approximated to solvent viscosity in diluted solutions otherwise suitable viscosity internal standards[8] can be chosen]. Further corrections to Equation (2) can also be made to account for shape factors or solute-to-solvent radii ratios.[9]

$$D = \frac{kT}{6\pi\eta R_H} \quad (2)$$

When complexation equilibria occur under fast-exchange conditions, the molecular sizes increase and the measured diffusion coefficient D_{obs}, which is the weighted average of its value in the bound (D_b) and free (D_f) forms, decreases to an extent that depends on complexed (x_b) and uncomplexed (x_f) molar fractions [Equation (3)].

$$D_{obs} = D_f x_f + D_b x_b \quad (3)$$

Self-association could lead to dimers, trimers or higher order aggregates, contributions of which can be evaluated by comparing the concentration dependence of diffusion coefficients. The diffusion parameters of the chiral auxiliaries **2**–**6** experienced small decreases on increasing the concentration from 5–25 mM, ranging from -0.12×10^{-10} $m^2 s^{-1}$ for **6** to -0.48×10^{-10} $m^2 s^{-1}$ for **2** (Table 6). On the same concentration gradient, the diffusion coefficient of underivatized quinine **1** decreased by -1.1×10^{-10} $m^2 s^{-1}$ (Table 6). Thus, carbamoylated derivatives of quinine were involved in self-aggregation equilibria to a lesser extent than underivatized quinine.

Table 6. Diffusion coefficients D [$10^{10} m^2 s^{-1}$] (600 MHz, $CDCl_3$, 25 °C) of **1**–**6** at different concentrations c_M.

c_M	**1**	**2**	**3**	**4**	**5**	**6**
5 mM	9.30	7.60	9.42	7.53	7.27	7.63
25 mM	8.20	7.12	9.26	7.32	7.11	7.51

With regard to chiral substrates **7**–**12** with the free carboxylic function, their tendency to form dimer species has already been demonstrated[10] and, in particular, a self-association constant of 161 ± 10 M^{-1} has been measured[10] for the derivative **7**, which means a dimer molar fraction of about 40% at 5 mM, which is very high. To establish whether chiral substrates interact with the chiral auxiliaries in their dimer or monomer forms, complexation stoichiometries were determined by Job's method[11] using the ^{19}F chemical shift measurements in mixtures of (*R*)-**7**/**4** and (*S*)-**7**/**4** at a constant total concentration (1 mM). Well-defined 1:1 stoichiometric ratios were found, which demonstrates that monomer enantiomeric substrates are solvated by chiral auxiliaries.

The diffusion coefficients of (*R*)-**7** and (*S*)-**7**, which were determined from ^{19}F NMR observations, decreased remarkably due to the presence of each chiral auxiliary (both derivatized and underivatized) and were slightly different

from each other with the sole exceptions of carbamate **5** and underivatized quinine **1**, neither of which were able to differentiate the enantiomers of **7** (Table 7). As an example, the diffusion coefficients of (*R*)-**7** and (*S*)-**7** (5 mM) decreased by -4.88×10^{-10} and -5.42×10^{-10} $m^2 s^{-1}$, respectively, in mixtures containing carbamate **4** (Table 7, Figure 10).

Table 7. A: Diffusion coefficients D [$10^{10} m^2 s^{-1}$] (564 MHz, $CDCl_3$, 25 °C) of pure **7** (5 mM) and in equimolar mixtures with **1**–**6**. B: The ratio between molar fractions in the bound state of the *R* (x_b^R) and the *S* (x_b^S) enantiomer of **7** in the mixture with **2**–**6**.

	7	**7/1**	**7/2**	**7/3**	**7/4**	**7/5**	**7/6**
A	11.93	7.59	7.42 (*R*)	8.13 (*R*)	6.51 (*R*)	7.23	7.43 (*R*)
A			6.59 (*S*)	7.53 (*S*)	7.05 (*S*)		6.78 (*S*)
B			0.84	0.86	0.90		0.87

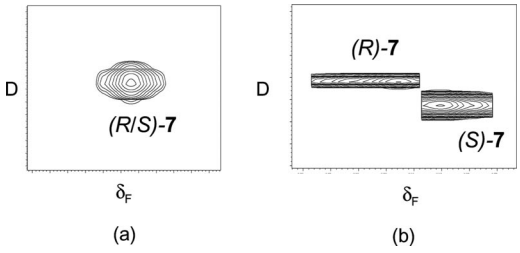

Figure 10. ^{19}F NMR DOSY map (564 MHz, $CDCl_3$, 25 °C, 5 mM) of the pure substrate **7** (a) and **7** in an equimolar mixture with **4** (b).

Thus large variations in the diffusion coefficients must be a consequence of very high molar fractions of complexed forms of both (*R*)-**7** and (*S*)-**7** in solution [Equation (3)] and hence the heteroassociation constants of diastereoisomeric complexes must be quite similar, but remarkably higher than their self-association constants. To confirm the above conclusion, the heteroassociation constants of the (*R*)-**7**/**4** and (*S*)-**7**/**4** complexes were determined by analysis of the ^{19}F chemical shifts of each enantiomer in solutions containing very large molar excesses (from 40:1 to 200:1) of **4** on the basis of Foster–Fyfe's method,[12] which was the most suitable one on consideration of the propensity of enantiomeric substrates to self-aggregation. Linear fittings of experimental data led to association constants of 233 ± 29 and 326 ± 36 M^{-1} for (*R*)-**7**/**4** and (*S*)-**7**/**4**, respectively, which were high and only slightly differentiated each other.

Diffusion coefficients of the other *N*-trifluoroacetylated amino acids (see Supporting Information, Table S4) underwent analogous decreases in the presence of chiral auxiliaries, but they were barely differentiated.

The remarkable sensitivity of the DOSY technique to complexation phenomena was confirmed in the case of the ester derivative of alanine **13**, the diffusion coefficient of which experienced a very small decrease in the presence of each chiral auxiliary (Table S4, Supporting Information), which illustrates the fact that very weak heteroaggregates are formed in these cases.

Owing to the fact that stabilities of diastereomeric solvents seemed to be quite similar, we explored the stereochemical basis of NMR anisochrony in mixtures (*R*)-**7**/**4** and (*S*)-**7**/**4**. The conformation of the carbamate derivative **4** was strongly perturbed as a consequence of the interaction with both (*R*)-**7** and (*S*)-**7** as its H8 proton was not only significantly high-frequency shifted, but it also became a singlet. Thus, the $^3J_{89}$ scalar vicinal coupling constant decreased to a value that was less than 2 Hz, which means that the Open(3) conformer, which is 37% of the total conformers in pure **4** (Table 5), became the most abundant in the presence of the two enantiomeric substrates. The H8–H9 ROE was more intense than the H8–H15 ROE (the contrary was true for pure **4**, Figure 7, a), in accord with the conformational change that occurs as a consequence of the interaction of the strongly basic quinuclidine nitrogen with the acidic carboxy group of each enantiomer of **7**. The amide moiety of (*R*)-**7** or (*S*)-**7** must contribute significantly to the stabilization of the two diastereoisomeric solvates as it undergoes remarkable high-frequency shifts (Table 1) due to the presence of the chiral auxiliary. The reasonably acidic amide group is itself involved in an attractive hydrogen-bond interaction with the carbonyl group or the oxygen atom of the carbamate moiety. The methyl and methine protons of the two enantiomers are in close proximity to the methoxy and H5 protons of **4**, as clearly witnessed by the dipolar interactions that originated in the two mixtures (Figures 11 and 12). The above findings led to the convergent picture of the two diastereoisomeric solvates given in Figure 13 in which the methyl and methine groups on the chiral centre of the amino acid derivative interchange their positions in (*R*)-**7** relative to (*S*)-**7**. In this way both the methyl and methine protons feel different shielding effects of the quinoline group, which are responsible for the NMR differentiation.

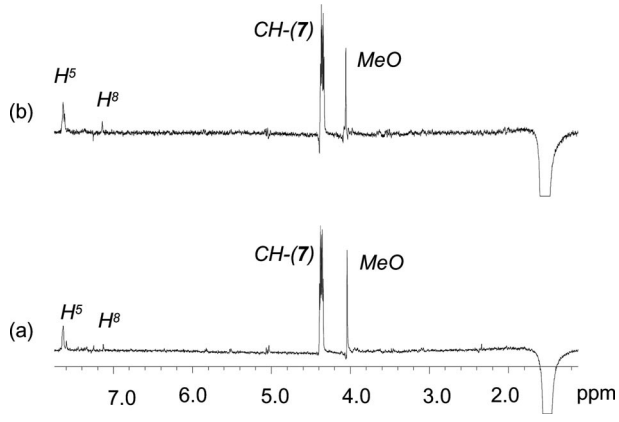

Figure 11. 1D ROESY spectra (600 MHz, $CDCl_3$, 60 mM, 25 °C, mix 0.6 s) corresponding to the selective inversion of the methyl nuclei of (*S*)-**7** (a) and (*R*)-**7** (b) in the presence of an equimolar amount of **4**.

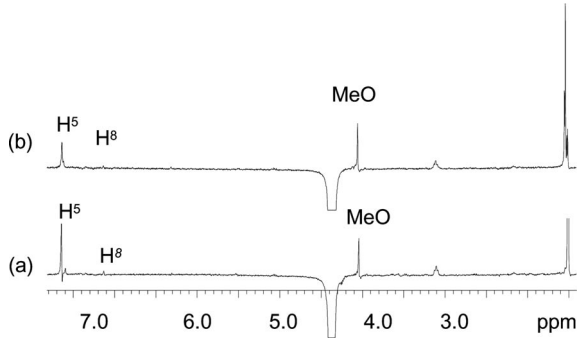

Figure 12. 1D ROESY spectra (600 MHz, $CDCl_3$, 60 mM, 25 °C, mix 0.6 s) corresponding to the selective inversion of the methine proton of (*S*)-**7** (a) and (*R*)-**7** (b) in the presence of an equimolar amount of **4**.

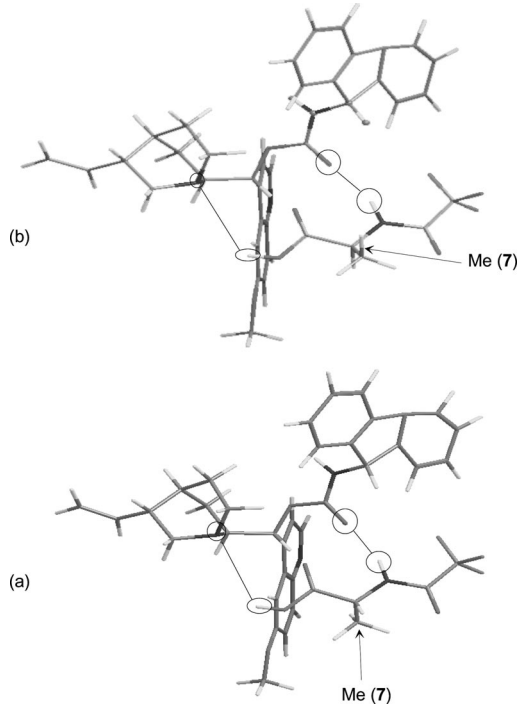

Figure 13. Graphical representation of the diastereoisomeric solvates formed in a solution of $CDCl_3$ (60 mM) by (*R*)-**7** (a) and (*S*)-**7** (b) with the **4**.

Conclusions

Quinine C^9-carbamoylation undoubtedly is a very practical way to obtain efficient and versatile chiral auxiliaries for NMR spectroscopy. The chiral recognition phenomena originated by this class of chiral auxiliary were rationalized by analysing the stereoelectronic effects of groups bound to the carbamate function. Moieties bound to the carbamate NH group mainly affect the relative populations of Closed to Open conformers. Bulky groups such as fluorenyl or trimethylsilyl are able to shift the conformational equilibria towards Open conformers in which the quinuclidine nitrogen is predisposed to interact with acidic functional groups, thereby enhancing enantiodiscrimination. As already established, the carbamate function OCONH attracts hydrogen-bonding donor groups of substrates more efficiently than the free hydroxy function. Two factors may contribute to this property: first, the self-aggregating propensity of quinine, which involves its hydroxy group, competes with substrate interactions and this effect is less pronounced for the carbamate derivatives, and secondly, the fact that a well-defined interaction pocket is created in carbamates inside which substrate interactions with the carbamate moiety are addressed and stereochemical differentiation of enantiomeric pairs can be enhanced.

Importantly, efficient enantiodiscrimination requires extensive cooperation between the carbamate NHCO function and another alkaloid functional group, as clearly demonstrated for *N*-trifluoroacetyl amino acid derivatives, which behave as bidentate ligands as their free carboxy function is able to interact efficiently with the strongly basic quinuclidine nitrogen atom. On this basis very stable diastereoisomeric solvates are formed in solution, the stereochemical differentiation of which can be detected at very low concentrations in spite of the fact that no significant degree of thermodynamic differentiation occurs.

A final remark concerns the great potential of the combined use of several NMR methods in fully comprehending chiral recognition processes at a molecular level: both thermodynamic and stereochemical aspects of diastereoisomeric supramolecular aggregation can be identified, which enables the rational design of chiral auxiliaries for use in several asymmetric processes.

Experimental Section

General Methods: ^1H, ^{19}F and ^{13}C NMR spectra were measured with a spectrometer operating at 600, 564 and 150 MHz, respectively. The temperature was controlled to within ±0.1 °C. All ^1H and ^{13}C NMR chemical shifts are referenced to TMS as the internal standard. ^{19}F NMR chemical shifts are referenced to trifluorotoluene as the external standard. The 2D NMR spectra were obtained by using standard sequences with the minimum spectral width required. Proton 2D gCOSY (*g*radient-*co*rrelated *s*pectroscop*y*) spectra were recorded with 256 increments of 4 scans and 2 K data points. The relaxation delay was 5 s. 2D TOCSY (*to*tal *c*orrelation *s*pectroscop*y*) spectra were recorded by employing a mixing time of 65 ms. The pulse delay was maintained at 5 s; 512 increments of 4 scans and 2 K data points each were collected. The 2D ROESY (*r*otating-frame *O*verhauser *e*nhancement *s*pectroscop*y*) experiments were performed in the phase-sensitive mode by employing a mixing time of 0.6 s. The pulse delay was maintained at 5 s; 256 increments of 4 scans and 2K data points each were collected. Proton 1D ROESY spectra were recorded by using selective pulses generated by the Varian Pandora Software. The selective 1D ROESY spectra were acquired with 1024 or 512 scans in 32 K data points with a 5 s relaxation delay and a mixing time ranging from 0.1 to 0.6 s.

The gradient ^1H,^{13}C gHSQC (*g*radient *h*eteronuclear *s*ingle *q*uantum *c*orrelation) and gHMBC (*g*radient *h*eteronuclear *m*ultiple *b*ond *c*orrelation) spectra were recorded with 512 or 256 time increments of 8 scans. The gradient HMBC experiments were optimized for a long-range ^1H–^{13}C coupling constant of 8 Hz and a delay period of 3.5 ms for the suppression of one-bond correlation signals. No decoupling was used during the acquisition.

DOSY (*d*iffusion *o*rdered *s*pectroscop*y*) experiments were carried out by using a stimulated echo sequence with self-compensating gradient schemes, a spectral width of 8000 Hz and 64 K data points. Typically, a value ranging from 100 to 180 ms was used for Δ, 1.0 ms for δ, and g was varied in 30 steps (from 2 to 512 transients each depending on the sample concentration) to obtain an approximately 90–95% decrease in resonance intensity at the largest gradient amplitudes. The baselines of all arrayed spectra were corrected prior to processing the data. After data acquisition, each FID was apodized with 1.0 Hz line-broadening and Fourier transformed. The data were processed with the DOSY macro (involving the determination of the resonance heights of all the signals above a pre-established threshold and the fitting of the decay curve for each resonance to a Gaussian function) to obtain pseudo-two-dimensional spectra with NMR chemical shifts along one axis and calculated diffusion coefficients along the other.

The stoichiometries for the two diastereoisomeric complexes (*R*)-**7**/**4** and (*S*)-**7**/**4** were determined by Job's method[11] by measuring the ^{19}F chemical shift of *N*-(trifluoroacetyl)alanine (**7**) in solutions prepared by mixing different volumes of stock solutions of each component having the same molar concentration (c_M) to obtain a prefixed volume directly in the NMR tube. Owing to the low solubility of **7**, the stoichiometry was determined on quite diluted solutions (c_M = 1 mM).

The heteroassociation constants for the two diastereoisomeric complexes (*R*)-**7**/**4** and (*S*)-**7**/**4** were determined by using the Foster–Fyfe method.[12] Linear fittings of the experimental data, obtained by analysis of the fluorine NMR spectra of solutions with increasing molar ratios of **4**/(*S*)- or (*R*)-**7** and a constant concentration of 0.1 mM for **7**, were performed.

Materials: 4-Phenoxyphenyl, 4-acetylphenyl, 3,4,5-trimethoxyphenyl, 9*H*-fluoren-9-yl and trimethylsilyl isocyanates, *N*-(trifluoroacetyl)alanine (**7**) and quinine (**1**) were purchased from Sigma–Aldrich.

Synthesis of Quinine Derivatives 2–6: The appropriate isocyanate (4.78 mmol) was added to a solution of **1** (4.62 mmol) in anhydrous toluene (60 mL) and then the reaction mixture was heated at reflux for 12 h. The solvent was removed in vacuo. The derivatives **2** and **4**–**6** were obtained in high yields (>90%) after purification by filtration through PTFE filters (45 μm). The derivative **3** was purified by chromatography on silica gel (acetone; 45% yield).

9-*O*-(3,4,5-Trimethoxyphenylcarbamoyl)quinine (2): Yield 2.39 g (97%). ^{1}H NMR (600 MHz, $CDCl_3$, 25 °C): δ = 1.54 (m, 1 H, 13-H), 1.59 (m, 1 H, 11-H), 1.71 (m, 1 H, 14-H), 1.84 (m, 1 H, 12-H), 1.88 (m, 1 H, 10-H), 2.27 (m, 1 H, 17-H), 2.63 (m, 1 H, 18-H), 2.65 (m, 1 H, 16-H), 3.03 (dd, $J_{19–18}$ = 13.2, $J_{19–17}$ = 10.1 Hz, 1 H, 19-H), 3.15 (m, 1 H, 15-H), 3.35 (m, 1 H, 9-H), 3.76 (s, 6 H, MeO[b]), 3.77 (s, 3 H, MeO[c]), 3.94 (s, 3 H, MeO), 4.99 (d, $J_{21–20}$ = 7.6 Hz, 1 H, 21-H), 5.01 (d, $J_{22–20}$ = 14.1 Hz, 1 H, 22-H), 5.82 (m, 1 H, 20-H), 6.51 (d, J_{89} = 7.3 Hz, 1 H, 8-H), 6.65 (s, 2 H, a-H), 7.20 (s, 1 H, NH), 7.33 (d, J_{12} = 4.2 Hz, 1 H, 1-H), 7.36 (dd, J_{43} = 9.4, J_{45} = 2.4 Hz, 1 H, 4-H), 7.48 (d, J_{54} = 2.4 Hz, 1 H, 5-H), 8.00 (d, J_{34} = 9.4 Hz, 1 H, 3-H), 8.70 (d, J_{21} = 4.2 Hz, 1 H, 2-H) ppm. ^{13}C NMR (150 MHz, $CDCl_3$, 25 °C): δ = 24.4 (C-7), 27.5 (C-5), 27.8 (C-4), 39.7 (C-3), 42.5 (C-6), 55.7 (MeO), 56.1 (C-27), 56.5 (C-2), 59.1 (C-8), 60.9 (C-29), 73.1 (C-9), 96.3 (C-25), 100.6 (C-18), 114.5 (C-11), 118.8 (C-15), 121.8 (C-20), 127.2 (C-17), 128.2 (C-24), 131.8 (C-21), 134.0 (C-28), 141.7 (C-10), 143.7 (C-16), 144.8 (C-22), 147.4 (C-14), 152.6 (C-23), 153.4 (C-26), 157.9 (C-19) ppm. $[a]_D^{25}$ = +32.6 (c = 1, $CHCl_3$).

9-*O*-(Trimethylsilylcarbamoyl)quinine (3): Yield 0.91 g (45%). ^{1}H NMR (600 MHz, $CDCl_3$, 25 °C): δ = 0.04 (s, 9 H, Me_3Si), 1.33 (1 H, 10-H), 1.49 (1 H, 14-H), 1.69 (1 H, 13-H), 1.79 (1 H, 12-H), 1.83 (1 H, 11-H), 2.24 (1 H, 17-H), 2.63 (1 H, 18-H), 2.68 (1 H, 15-H), 2.95 (1 H, 9-H), 3.10 (1 H, 19-H), 3.47 (1 H, 16-H), 3.93 (3 H, MeO), 4.87 (br. s, 1 H, 21-H), 4.92 (d, $J_{22–20}$ = 17.2 Hz, 1 H, 22-H), 5.67 (br. s, 1 H, 8-H), 5.72 (m, 1 H, 20-H), 7.19 (br. s, 1 H, 5-H), 7.36 (d, J_{43} = 9.1 Hz, 1 H, 4-H), 7.48 (1 H, 1-H), 7.49 (br. s, 1 H, NH), 8.01 (d, J_{34} = 9.1 Hz, 1 H, 3-H), 8.72 (br. s, 1 H, 2-H) ppm. ^{13}C NMR (150 MHz, $CDCl_3$, 25 °C): δ = 0.2 (Me_3Si), 20.7 (C-7), 27.7 (C-5), 27.9 (C-4), 40.1 (C-3), 43.3 (C-6), 55.7 (MeO), 57.6 (C-2), 60.9 (C-8), 73.1 (C-9), 100.6 (C-18), 114.2 (C-11), 118.7 (C-15), 121.5 (C-20), 131.8 (C-21), 142.5 (C-10), 144.4 (C-22), 147.4 (C-14), 126.3/147.7 (C_{16}/C_{17}), 157.9 (C_{19}/C_{23}) ppm. $[a]_D^{25}$ = –141.9 (c = 1, $CHCl_3$).

9-*O*-(9*H*-Fluoren-9-ylcarbamoyl)quinine (4): Yield 2.31 g (94%). ^{1}H NMR (600 MHz, $CDCl_3$, 25 °C): δ = 1.56 (m, 1 H, 13-H), 1.63 (1 H, 11-H), 1.75 (m, 1 H, 14-H), 1.87 (m, 2 H, 10- and 12-H), 2.28 (m, 1 H, 17-H), 2.63 (m, 1 H, 18-H), 2.72 (m, 1 H, 16-H), 3.07 (dd, $J_{19–18}$ = 13.3, $J_{19–17}$ = 10.8 Hz, 1 H, 19-H), 3.21 (m, 1 H, 15-H), 3.34 (m, 1 H, 9-H), 3.97 (s, 3 H, MeO), 4.97 (d, $J_{21–20}$ = 9.2 Hz, 1 H, 21-H), 5.00 ($J_{22–20}$ = 18.1 Hz, 1 H, 22-H), 5.21 (d, $J_{NH–a}$ = 9.4 Hz, 1 H, NH), 5.81 (m, 1 H, 20-H), 5.85 (d, $J_{a–NH}$ = 9.4 Hz, 1 H, a-H), 6.60 (d, J_{89} = 6.6 Hz, 1 H, 8-H), 7.21 (dd, $J_{c′d′}$=$J_{c′e′}$=7.3 Hz,1 H, c′-H), 7.33 (m, 2 H, b′-H and c-H), 7.36 (dd, $J_{d′e′}$= 7.5, $J_{d′c′}$=7.3 Hz, 1 H, d′-H), 7.38 (d, J_{12}=3.9 Hz, 1 H, 1-H), 7.40 (m, 2 H, 4-H and d-H), 7.53 (d, J_{54}=2.7 Hz, 1 H, 5-H), 7.62 (d, J_{bc} = 7.0 Hz, 1 H, b-H), 7.65 (d, $J_{e′–d′}$ = 7.5 Hz, 1 H, e'-H), 7.68 (d, J_{ed} = 7.7 Hz, 1 H, e-H), 8.03 (d, J_{34} = 9.6 Hz, 1 H, 3-H), 8.74 (d, J_{21} = 3.9 Hz, 1 H, 2-H) ppm. ^{13}C NMR (150 MHz, $CDCl_3$, 25 °C): δ = 24.0 (C-7), 27.6 (C-4), 27.8 (C-5), 39.8 (C-3), 42.6 (C-6), 55.7 (MeO), 56.6 (C-2), 56.7 (C-24), 59.3 (C-8), 74.7 (C-9), 101.5 (C-18), 114.5 (C-11), 118.6 (C-15), 119.9/120.0 (C-29/C-29′), 121.8 (C-20), 124.9/125.3 [C-26/C-26′(C-27)], 127.2 (C-17), 127.8/128.2 [C-27′/C-27(C-26′)], 128.8/129.0 (C-28/C-28′), 131.8 (C-21), 140.3/140.4/143.8/144.8 (C-25/C-25′/C-30/C-30′), 141.8 (C-10), 144.0/144.1 (C-16/C-22), 147.5 (C-14), 156.5 (C-23), 157.9 (C-19) ppm. $[a]_D^{25}$ = –16.2 (c = 1, $CHCl_3$).

9-*O*-(4-Phenoxyphenylcarbamoyl)quinine (5): Yield 2.27 g (92%). ^{1}H NMR (600 MHz, $CDCl_3$, 25 °C): δ = 1.54 (m, 1 H, 13-H), 1.60 (m, 1 H, 11-H), 1.74 (m, 1 H, 14-H), 1.88 (br. s, 1 H, 12-H), 1.95 (m, 1 H, 10-H), 2.29 (m, 1 H, 17-H), 2.65 (m, 1 H, 18-H), 2.66 (m, 1 H, 16-H), 3.05 (dd, $J_{19–18}$ = 13.5, $J_{19–17}$ = 10.3 Hz, 1 H, 19-H), 3.13 (m, 1 H, 15-H), 3.41 (m, 1 H, 9-H), 3.96 (s, 3 H, MeO), 5.01 (d, $J_{21–20}$ = 7.9 Hz, 1 H, 21-H), 5.04 (d, $J_{22–20}$ = 15.5 Hz, 1 H, 22-H), 5.86 (m, 1 H, 20-H), 6.53 (d, J_{89} = 8.3 Hz, 1 H, 8-H), 6.84 (br. s, 1 H, NH), 6.94 (2 H, c-H), 6.97 (2 H, b-H), 7.06 (t, 1 H, e-H), 7.30 (2 H, d-H), 7.31 (2 H, a-H), 7.37 (d, J_{43} = 8.9 Hz, 1 H, 4-H), 7.41 (d, J_{12} = 4.4 Hz, 1 H, 1-H), 7.49 (br. s, 1 H, 5-H), 8.01 (d, J_{34} = 8.9 Hz, 1 H, 3-H), 8.76 (d, J_{21} = 4.4 Hz, 1 H, 2-H) ppm. ^{13}C NMR (150 MHz, $CDCl_3$, 25 °C): δ = 24.5 (C-7), 27.5 (C-5), 27.8 (C-4), 39.7 (C-3), 42.4 (C-6), 55.7 (MeO), 56.5 (C-2), 59.1 (C-8), 74.0 (C-9), 101.5 (C-18), 114.5 (C-11), 118.3 (C-29), 118.9 (C-15), 119.8 (C-26), 120.3 (C-25), 121.8 (C-20), 123.0 (C_{31}), 127.3 (C-17), 129.7 (C-30), 131.8 (C-21), 133.0 (C-24), 141.8 (C-10), 143.7 (C-16), 144.8 (C-22), 147.5 (C-14), 152.9 (C-23), 153.1/157.7 (C-27/C-28), 157.7 (C-19) ppm. $[a]_D^{25}$ = –58.6 (c = 1, $CHCl_3$).

9-*O*-(4-Acetylphenylcarbamoyl)quinine (6): Yield 2.04 g (91%). ^{1}H NMR (600 MHz, $CDCl_3$, 25 °C): δ = 1.57 (m, 1 H, 13-H), 1.58 (m, 1 H, 11-H), 1.74 (m, 1 H, 14-H), 1.88 (br. s, 1 H, 12-H), 1.96 (m, 1 H, 10-H), 2.29 (m, 1 H, 17-H), 2.54 (s, 3 H, c-H), 2.64 (m, 1 H, 18-H), 2.66 (m, 1 H, 16-H), 3.05 (dd, $J_{19–17}$ = 10.6, $J_{19–18}$ = 13.3 Hz, 1 H, 19-H), 3.12 (m, 1 H, 15-H), 3.41 (m, 1 H, 9-H), 3.96 (s, 3 H, MeO), 5.02 (d, $J_{21–20}$ = 9.4 Hz, 1 H, 21-H), 5.04 (d, $J_{22–20}$ =

16.4 Hz, 1 H, 22-H), 5.86 (m, 1 H, 20-H), 6.54 (d, J_{89} = 7.5 Hz, 1 H, 8-H), 7.19 (br. s, 1 H, NH), 7.37 (dd, J_{43} = 9.4, J_{45} = 2.2 Hz, 1 H, 4-H), 7.38 (d, J_{12} = 4.2 Hz, 1 H, 1-H,), 7.45 (d, J_{ab} = 8.6 Hz, 2 H, a-H), 7.49 (d, J_{54} = 2.2 Hz, 1 H, 5-H), 7.89 (d, J_{ba} = 8.6 Hz, 2 H, b-H), 8.01 (d, J_{34} = 9.4 Hz, 1 H, 3-H), 8.74 (d, J_{21} = 4.2 Hz, 1 H, 2-H) ppm. ^{13}C NMR (150 MHz, $CDCl_3$, 25 °C): δ = 24.7 (C-7), 26.4 (C-29), 27.4 (C-4), 27.8 (C-5), 39.6 (C-3), 42.4 (C-6), 55.7 (MeO), 56.4 (C-2), 59.1 (C-8), 74.4 (C-9), 101.5 (C-18), 114.6 (C-11), 117.7 (C-25), 118.9 (C-15), 121.8 (C-20), 127.3 (C-17), 129.8 (C-26), 131.8 (C-21), 132.5 (C-27), 141.7 (C-10), 141.9 (C-24), 143.4 (C-16), 144.8 (C-22), 147.4 (C-14), 152.3 (C-23), 158.1 (C-19), 196.8 (C-28) ppm. $[\alpha]_D^{25}$ = +48.3 (c = 1, $CHCl_3$).

Supporting Information (see also the footnote on the first page of this article): ^{1}H non-equivalences (600 MHz) measured for the protons of **9**–**11** (5 mM) in presence of equimolar amounts of **3** and **4**. ^{19}F non-equivalences (564 MHz) measured for **7**–**11** in the presence of equimolar amounts of CSAs. Diffusion coefficients of **8**–**11** and **13**, pure and in equimolar mixtures, with **1**–**6**. 1D ROESY spectra corresponding to the saturation of the H8 proton of **4** and **6**.

Acknowledgments

This work was supported by the Ministero dell'Università e della Ricerca and Fondo per gli Investimenti della Ricerca di Base (FIRB), Project RBPR05NWWC.

[1] a) C. O. Dalaigh, *Synlett* **2005**, 875–876; b) S.-K. Tian, Y. Chen, J. Hang, L. Tang, P. McDaid, L. Deng, *Acc. Chem. Res.* **2004**, *37*, 621–631; c) K. Kacprzak, J. Gawronski, *Synthesis* **2001**, *7*, 961–998.

[2] a) G. Uccello-Barretta, F. Balzano, C. Quintavalli, P. Salvadori, *J. Org. Chem.* **2000**, *65*, 3596–3602; b) G. Uccello-Barretta, S. Bardoni, F. Balzano, P. Salvadori, *Tetrahedron: Asymmetry* **2001**, *12*, 2019–2023; in Figure 1 the structures of **1e** and **1f** were interchanged: c) G. Uccello-Barretta, F. Mirabella, F. Balzano, P. Salvadori, *Tetrahedron: Asymmetry* **2003**, *14*, 1511–1516; d) G. Uccello-Barretta, F. Balzano, P. Salvadori, *Chirality* **2005**, *17*, S243–S248; e) A. Maly, B. Lejczak, P. Kafarski, *Tetrahedron: Asymmetry* **2003**, *14*, 1019–1024; f) M. Abid, B. Toeroek, *Tetrahedron: Asymmetry* **2005**, *16*, 1547–1555.

[3] a) N. M. Maier, W. Lindner in *Methods and Priciples in Medicinal Chemistry*, vol. 33, *Chirality in Drug Research* (Eds.: E. Francotte, W. Lindner), Wiley-VCH, Weinheim, Germany, **2006**, chapter 7; b) M. Lammerhofer, P. Franco, W. Lindner, *J. Sep. Sci.* **2006**, *29*, 1486–1496; c) M. Lammerhofer, W. Lindner, *Adv. Chromatogr.* **2008**, *46*, 1–107.

[4] a) C. S. Johnson, *Prog. Nucl. Magn. Reson. Spectrosc.* **1999**, *34*, 203–256; b) T. Brand, E. J. Cabrita, S. Berger, *Prog. Nucl. Magn. Reson. Spectrosc.* **2005**, *46*, 159–196.

[5] T. Burgi, A. Baiker, *J. Am. Chem. Soc.* **1998**, *120*, 12920–12926.

[6] a) M. Karplus, *J. Chem. Phys.* **1959**, *30*, 11–15; b) M. Karplus, *J. Am. Chem. Soc.* **1963**, *85*, 2870–2871; c) G. Govil, R. V. Hosur in *NMR: Basic Principles and Progress, Conformation of Biological Molecules: Results from NMR*, Springer, New York, **1982**, vol. 20.

[7] G. Uccello-Barretta, L. Di Bari, P. Salvadori, *Magn. Reson. Chem.* **1992**, *30*, 1054–1063.

[8] E. J. Cabrita, S. Berger, *Magn. Reson. Chem.* **2001**, *39*, S142–S148.

[9] a) L. Allouche, A. Marquis, M. J. Lhen, *Chem. Eur. J.* **2006**, *12*, 7520–7525; b) D. Zuccaccia, A. Macchioni, *Organometallics* **2005**, *24*, 3476–3486; c) K. Z. Wirtz, *Z. Naturforsch., Teil A* **1953**, *8*, 532–538; d) A. Giere, K. Z. Wirtz, *Z. Naturforsch., Teil A* **1953**, *8*, 522–532.

[10] G. Uccello-Barretta, F. Balzano, F. Pertici, L. Jicsinszky, G. Sicoli, V. Schurig, *Eur. J. Org. Chem.* **2008**, *11*, 1855–1863.

[11] a) P. Job, *Justus Liebigs Ann. Chem.* **1928**, *9*, 113–134; b) J. Homer, M. Perry, *J. Chem. Soc. Faraday Trans. 1* **1986**, *82*, 533–543.

[12] L. Fielding, *Tetrahedron* **2000**, *56*, 6151–6170.

Received: October 14, 2008
Published Online: January 8, 2009

